Crystal Structure and Morphology of Poly(L-lactide-*b*-D-lactide) Diblock Copolymers

Liangbin Li,*,† Zhiyuan Zhong,‡ Wim H. de Jeu,† Pieter J. Dijkstra,‡ and Jan Feijen‡

FOM-Institute for Atomic and Molecular Physics, Kruislaan 407, 1098 SJ Amsterdam, The Netherlands, and Department of Polymer Chemistry and Biomaterials and Institute for Biomedical Technology, Faculty of Science and Technology, University of Twente, 7500 AE, Enschede, The Netherlands

Received May 11, 2004; Revised Manuscript Received September 2, 2004

ABSTRACT: The isothermal crystallization behavior of low-molecular-weight (DP ≅ 50) poly(L-lactide-*b*-D-lactide) diblock copolymers is reported, as studied by small- and wide-angle X-ray scattering. The symmetric diblock copolymer crystallizes in the stereocomplex form for the whole range of crystallization temperatures, while the one with a block ratio of 80/20 grows into homocrystallites. For an intermediate block ratio (66/33), the stereocomplex form is obtained at high crystallization temperatures while a coexistence region with homocrystal phase exists at low temperatures. In addition to the transition enthalpy, size effects and kinetic routes play a role in the competition between the stereocomplex and the homocrystalline forms. The lamellar spacing (long period and crystal thickness) shows a different temperature dependence for the three diblock copolymers, which is discussed in relation to the specific morphology and molecular constitution.

Introduction

To achieve a better understanding of the crystallization process and the resulting final structure of polymers, many types of model system have been employed.[1] Integer as well as noninteger folded-chain crystals have been observed for polymers with low molecular weight and narrow polydispersity.[2,3] A specific functional group, for instance, the amide group in the nylon family, enables the study of the fold and lateral surface of lamellar crystals.[4] So-called self-poisoning has been found in blends of monodisperse *n*-alkanes.[5] Studies on other model systems such as block copolymers,[6−9] branched oligomers,[10,11] and cyclic oligomers[12,13] also contribute to a better understanding of polymer crystallization. Stereocomplex crystals provide another model system for studying solid solubility, chain selection processes, and chain folding.[14,15] A typical example is the stereocomplex form of polylactides (PLA's), which has been systematically studied so far in blends of poly(L-lactide) (PLLA) and poly(D-lactide) (PDLA).[16−22]

PLA's are among the most important biodegradable synthetic polymers of interest for medical applications such as controlled drug delivery, resorbable sutures, medical implants, and scaffolds for tissue engineering.[23] On the basis of annually renewable resources like corn and sugar beets, PLA's are promising degradable substitutes for petrochemical-based polyolefins.[24] Because of the presence of a chiral center, PLA properties can be varied by changing the enantiomeric composition.[16−22] Amorphous, homocrystalline, and stereocomplex (racemic) states can be obtained by controlling the chain stereochemistry. Since the early investigations by Fischer et al.,[25] several groups have studied the crystallization behavior of PLA's, especially the stereocomplex form.[16−22] In blends of poly(L-lactide) (PLLA) and poly(D-lactide) (PDLA), the two molecular species can crystallize into a 1/1 stereocomplex with a melting point 50 °C above that of the enantiomeric components.[16] In stereocomplex crystallites each molecular species adopts a specific helical hand, imposed by the stereochemistry: left-handed for PLLA and right-handed for PDLA. In equimolar blends the two molecular species can also crystallize separately in different crystallites (homocrystallites). This situation may be changed when the two species are covalently connected with each other as in diblock copolymers. We anticipate that in a diblock copolymer of PLLA and PDLA,[26−29] where the two blocks only differ in configurations, the competition between racemic and homocrystallizations may bring out some interesting phenomena.

In this work, the crystallization behavior of diblock copolymers poly(L-lactide-*b*-D-lactide) with different ratios of the chain length of the two blocks is investigated with in-situ small- and wide-angle X-ray scattering. In the case of the symmetric block copolymer (50/50), stereocomplex crystals are obtained over the whole range of crystallization temperatures. The highly asymmetric block copolymer (80/20) only crystallizes in homocrystals with noninteger folds. The intermediate example (66/33) shows the stereocomplex at high and the homocrystalline form at low crystallization temperatures.

Experimental Section

Materials. Diblock copolymers, poly(L-lactide-*b*-D-lactide), were prepared by sequential polymerization of L-lactide and D-lactide monomers using 2-propanol−$Ca[N(SiMe_3)_2]_2(THF)_2$ as an initiating system, with polymerization conditions similar as reported previously.[30−32] The molar ratios between L-lactide and D-lactide in the studied three copolymers are 80/20, 66/33, and 50/50, respectively; they will be denoted as LD80/20, LD66/33, and LD50/50. ^{1}H NMR end group analysis and GPC indicated that all polymers have a degree of polymerization of about 50 and a polydispersity around 1.05 (see Table 1). For these low molecular weights in the melt no microphase separation is expected.

† FOM-Institute for Atomic and Molecular Physics.
‡ University of Twente.
* Corresponding author: e-mail liangbin@amolf.nl.

10.1021/ma049077o CCC: $27.50
Published on Web 10/16/2004

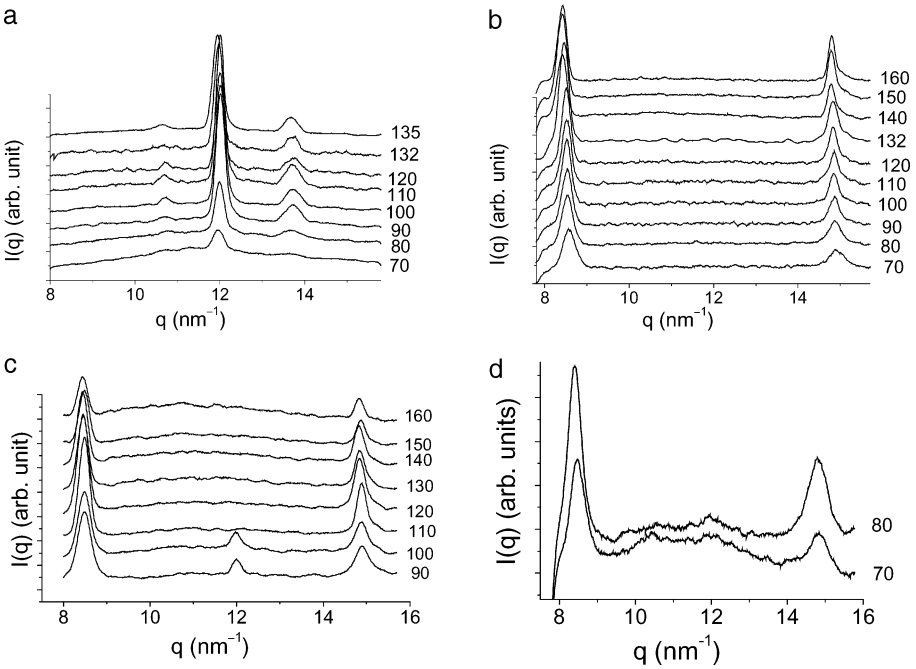

Figure 1. WAXS patterns of poly(L-lactide-*b*-D-lactide) diblock copolymers isothermally crystallized at the different temperatures indicated: (a) LD80/20; (b) LD50/50; (c, d) LD66/33.

Table 1. Molecular Parameters of Poly(L-lactide-*b*-D-lactide) Block Copolymers

copolymer	DP$_{^1H\ NMR}$	$M_{n\ GPC}$	M_w/M_n
LD80/20	52	7800	1.07
LD66/33	49	7400	1.05
LD50/50	53	7700	1.04

Characterization. Simultaneous WAXS and SAXS measurements were made using an in-house setup with a rotating anode X-ray generator (Rigaku RU-H300, 18 kW) equipped with two parabolic multilayer mirrors (Bruker, Karlsruhe), giving a highly parallel beam (divergence about 0.012°) of monochromatic Cu Kα radiation ($\lambda = 0.154$ nm). The SAXS intensity was collected with a two-dimensional gas-filled wire detector (Bruker Hi-Star). A semitransparent beamstop placed in front of the area detector allowed monitoring the intensity of the direct beam. The WAXS intensity was recorded with a linear position-sensitive detector (PSD-50M, M. Braun, Germany), which could be rotated around the beam path to measure either in the meridianal or in the equatorial direction. The SAXS and WAXS intensities were normalized to the intensity of the direct beam.

Experimental Procedure. A Linkam CSS450 temperature-controlled shear system was employed as sample stage. Samples were kept in a brass sample holder with Kapton windows replacing the original glass windows of the system. For isothermal crystallization the sample was first heated to 210 °C for 10 min and subsequently cooled to the crystallization temperature. The temperature of 210 °C is sufficient to melt the crystals as the low molecular weight reduces the melting point of stereocomplex form from normally 230 °C in blends[16−18] and 205 °C in long-chains copolymers[26] to around 190 °C in present materials. A nitrogen atmosphere prevented possible degradation at high temperatures. SAXS and WAXS measurements were taken during isothermal crystallization with 30 and 120 s per frame, respectively. After completion of the crystallization, as indicated by saturation of the SAXS intensity, a 20 min measurement was taken to obtain high-quality statistics.

Data Analysis. The two-dimensional SAXS intensity was first integrated azimuthally to obtain the scattering pattern as a function of $q = 4\pi \sin\theta/\lambda$, the modulus of the momentum transfer vector **q**, λ being the X-ray wavelength and 2θ the scattering angle. To examine the lamellar structures, linear correlation functions $\gamma(r)$[33−35] were calculated according to

$$\gamma(r) = \frac{1}{Q}\int_0^\infty I(q)q^2 \cos(qr)\, dq \quad (1)$$

$$Q = \int_0^\infty I(q)q^2\, dq \quad (2)$$

where Q is the so-called invariant. The correlation functions contain the basic morphological information for a model of lamellar stacks. The long spacing L can be estimated from the position of the first maximum. Further analysis of the correlation function yields the average crystalline lamellar thickness l_c and the amorphous layer thickness l_a. From these results the linear crystallinity $\phi_{cl} = l_c/L$ within the stacks can be calculated. However, analysis of the correlation function alone cannot tell which value of a subspacing belongs to l_c and which to l_a. We choose to assign the larger one to l_c on the basis of the ratio between the length of two blocks.

Results and Discussion

Crystal Structure. Figure 1 shows the WAXS curves of the three poly(L-lactide-*b*-D-lactide) samples isothermally crystallized at different temperatures. The highly asymmetric diblock copolymer LD80/20 only crystallizes in a homocrystalline structure (Figure 1a), which has a melting temperature around 145 °C. The highest crystallization temperature chosen is 135 °C, which takes 4 days for completion of the crystallization. The homocrystals are in the α phase; the β form of PLLA is only obtained under special condition such as shear flow.[36] The symmetric diblock copolymer LD50/50 leads only to the stereocomplex form for the whole range of crystallization temperatures up to 170 °C (Figure 1b). At an intermediate ratio between the two blocks, LD66/33 shows different results for two crystallization temperature regions (Figure 1c,d). At temperatures above 110 °C, LD66/33 grows in the stereocomplex form, while both homocrystals and the stereocomplex phase occur at lower temperatures. Here again the homocrystals are in the α phase. Similar phenomena occur for blends from L-lactide rich and D-lactide rich PLAs.[27] As at temper-

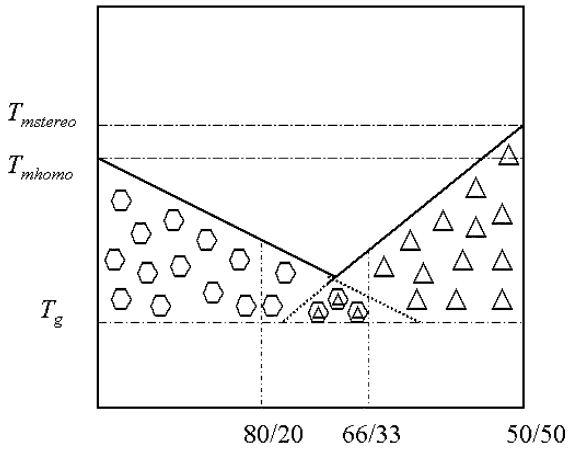

Figure 2. Schematic phase diagram of poly(L-lactide-*b*-D-lactide) diblock copolymers (composition vs temperature). Hexagons and triangle represent the homocrystallites and the stereocomplex form, respectively.

atures of 70 and 80 °C the WAXS peak of the homocrystals is very weak; they are shown separately in Figure 1d on a different intensity scale.

On the basis of the WAXS results of the three samples at different temperatures, a schematic phase diagram of poly(L-lactide-*b*-D-lactide) can be drawn as given in Figure 2. At large asymmetry the block copolymer can only crystallize in homocrystallites, while only stereocomplex crystals are obtained in the sample with symmetric blocks. The two crystalline forms have a coexistence region that depends on the ratio between the lengths of two blocks as well as on temperature.

Lamellar Morphology. Figure 3a shows a typical one-dimensional SAXS intensity curve of an isothermally crystallized poly(L-lactide-*b*-D-lactide) diblock copolymer. On the basis of the SAXS measurements and eq 1, we calculate the one-dimensional density correlation function of Figure 3b. The latter figure also demonstrates the deduction of the morphological parameters: the long period L and the crystal thickness l_c. We shall now give the detailed results for the three cases.

Sample LD50/50. Figure 4a gives the morphology parameters of the LD50/50 isothermally crystallized at different temperatures as obtained from the correlation functions. The long period L and crystal thickness l_c increase linearly with temperature. According to NMR results, this block copolymer contains 53 lactide monomers (106 lactic acid monomers). The length of the extended chain is approximately 31 nm with the 3/1 conformation in the stereocomplex triclinic or trigonal unit cell.[19] Because the ratio between the L-lactide and D-lactide blocks is 50/50, the two blocks have the same length of about 15.5 nm. For such a relatively short molecular length, polymers generally show a preference for integer folding, leading to a stepwise increase of crystal thickness with crystallization temperatures.[1] However, in the present system a continuous increase of crystal thickness is observed with temperature. The temperature dependence of crystal thickness follows the general behavior of high-molecular-weight homopolymers: l_c is inversely proportional to the suppercooling $\Delta T = T_m^o - T_c$ and T_m^o and T_c are the equilibrium melting point and crystallization temperature, respectively.[37] In the stereocomplex crystals, the racemic lattice requires D-lactide and L-lactide chains to pack side-by-side in a 1:1 ratio, which reduces the possibility

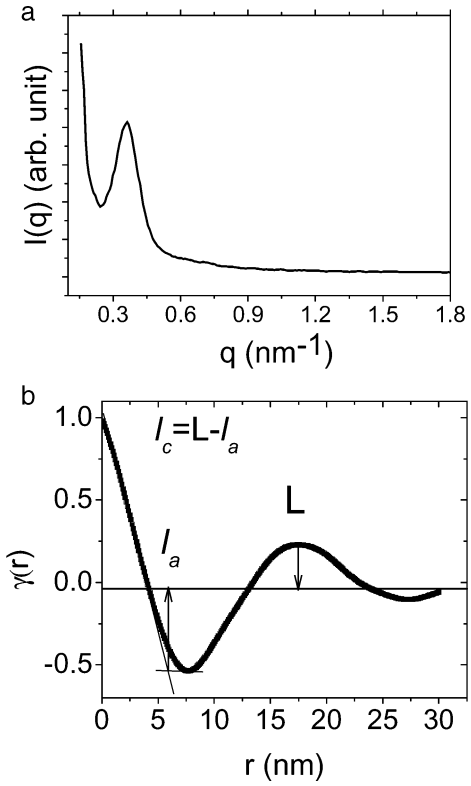

Figure 3. SAXS results for a isothermally crystallized poly(L-lactide-*b*-D-lactide) diblock copolymer LD66/33 at 130 °C: (a) typical one-dimensional SAXS pattern; (b) corresponding correlation function. L, l_c, and l_a denote the long period, the crystal thickness, and the interlamellar amorphous thickness, respectively.

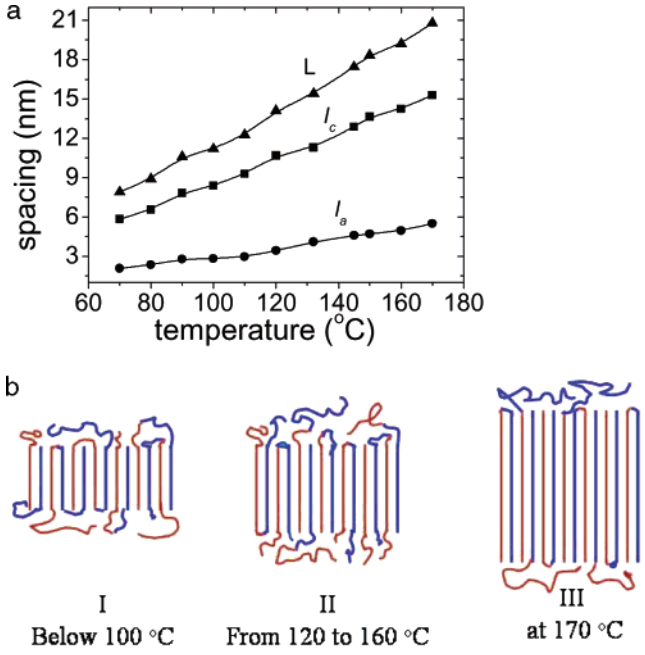

Figure 4. (a) Morphological parameters of LD50/50 isothermally crystallized at different temperatures. (b) Schematic picture of the lamellar crystals.

of adjacent reentrance and tight folds.[18] If there are any tight folds on the surface of the crystals, the only possibility for such a fold is the junction between the two blocks. This may be one of the reasons to prevent LD50/50 molecules from folding into four stems. If this would occur, a constant crystal thickness of about 7.8 nm should appear at temperatures around 90 °C.

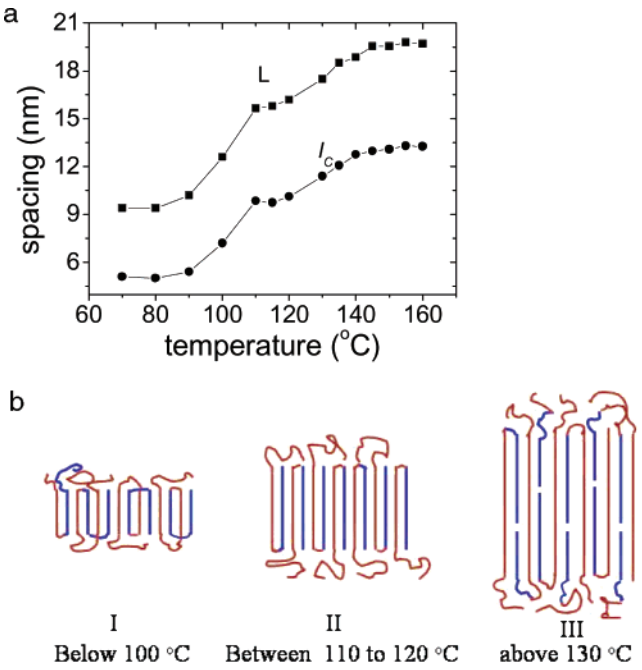

Figure 5. (a) Morphological parameters of LD66/33 isothermally crystallized at different temperatures. (b) Schematic picture of the lamellar crystals.

Moreover, in the case of integer folds, the thickness of the amorphous layer would be much smaller.

It seems more appropriate to treat LD50/50 simply as a homopolymer with a molecular length of 31 nm rather than as a diblock copolymer with two block lengths of 15.5 nm. Figure 4b shows schematic pictures of the crystals at different temperatures. Quite generally, interlamellar amorphous layers are occupied by loops, cilia, and tie chains. Comparing the morphological parameters and the length of the molecular chains, we notice that these three components play different roles in different temperature regions. At a temperature below 100 °C (Figure 4b-I), the crystal thickness is less than $^1/_4$ of the total chain length. This offers many possibilities to assemble the molecular chains. Hence, loops, cilia, and tie chains have the same probability to appear in the amorphous layers. At temperature above 120 °C (Figure 4b-II), the long period is already larger than half the molecular length. Now tight loops with low entropy are unfavorable, and cilia can be expected to play a more important role in filling the amorphous layers. At 170 °C (Figure 4b-III), the crystal thickness is about equal to the length of each block and cilia completely dominate the amorphous layers.

Sample LD66/33. Figure 5a shows the long period and lamellar crystal thickness of LD66/33 isothermally crystallized at different temperatures. Both the long period and the crystalline thickness show relatively constant values in three different temperature regions. From 110 to 120 °C the crystal thickness of LD66/33 is close to 9.7 nm, approximately the length of the D-lactide block. The total D-lactide block incorporates about half the L-lactide block to form the stereocomplex crystal (Figure 5b-II). In this case, the crystallization leaves the other half of the L-lactide—rather than the total D-lactide block—in the interlamellar amorphous layers, even though both have the same length. At the low-temperature side of this temperature region, the lamellar spacing (long period and crystal thickness) shows a sharp decrease. The crystal thickness has a relative

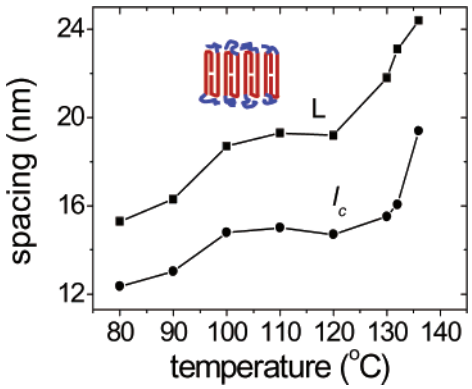

Figure 6. Morphological parameters of LD80/20 isothermally crystallized at different temperatures. The inset indicates crystals with one and half stems in the temperature range between 100 and 120 °C.

constant value around 5 nm, which is now about half of the length of D-lactide. This suggests that in this temperature range crystals form with 1-fold of D-lactide block (see Figure 5b-I). One could also argue that the sharp decrease of the lamellar spacing is due to the formation of both stereocomplex and homocrystal layers within the same domains. If half of the L-lactide block crystallizes with D-lactide in the stereocomplex form and another half organizes in homocrystals, the long period also should show a sharp decrease. However, then we expect in addition an increase of the linear crystallinity, which is not observed. Moreover, at 70 and 80 °C, the crystalline peak of the homocrystals is rather weak compared to that of the stereocomplex. This implies that the two crystalline forms indeed crystallize separately. Finally, at high temperatures, though the lamellar spacing continuously increases with increasing crystallization temperature, the slope saturates. We cannot assign this nearly constant crystal thickness of 13.3 nm to any integer fold because the total length of the D-lactide block is about 10 nm. The formation of crystals with a thickness larger than the length of a single block must originate from contributions of two D-lactide blocks from different macromolecules (Figure 5b-III). The slowing down of the increase of the lamellar spacing is possibly due to the entropy loss of the L-lactide in the melt.

Sample LD80/20. The morphological parameters of LD80/20 crystallized at different temperatures are plotted in Figure 6. Similar to the result for LD66/33, lamellar crystals with a constant value about 14.8 nm exists at temperatures from 100 to 130 °C. Because LD80/20 forms homocrystals, only L-lactide blocks take part in the crystallization. The L-lactide block in LD80/20 has a length of about 24 nm, assuming it to be in a 10/7 helix conformation. A comparison of the crystal thickness and the length of the L-lactide block indicates that the lamellae with a constant thickness of about 14.8 nm are not integer-fold crystals. The ratio between chain length and crystal thickness is close to 1.6. A schematic picture of lamellar crystals with 1.5-fold of the L-lactide block is given in Figure 6.

General Discussion. The appearance of the stereocomplex and/or the homocrystals is not only determined by thermodynamics but also influenced by kinetic competition. In principle, the formation of homocrystals means that D-lactide blocks are pushed away from the growth front. Hence, kinetically we expect it to be more difficult for homocrystals to form than for the stereo-

complex phase, especially at temperatures close to the glass transition. This is reflected in the WAXS patterns of LD66/33 at 70 °C, in which the peak from the homocrystals is much weaker than that at 100 °C.

For relatively short chain length, even thermodynamic competition alone between the stereocomplex and homocrystalline forms is already rather complicated. The different cohesion energy of the unit cell (thermal enthalpy) may be (over)compensated by size effects.[38] Let us follow the Hoffman−Weeks[39] formulation for the melting point $T_m = T_m^o(1 - 2\sigma_e/l\Delta H)$, in which T_m^o is the equilibrium melting temperature, l the lamellar thickness, ΔH the enthalpy, and σ_e the folded-chain surface free energy. The relative stability of the stereocomplex and the homocrystalline forms can be inverted by a change in the lamellar thickness, even though T_m and ΔH for the stereocomplex form are larger than for homocrystals. This happens in the case of LD80/20, which crystallizes only in the homocrystalline form: homocrystallites with a minimum thickness larger than 12 nm are more stable than the stereocomplex form with a lamellar thickness less than 6 nm.

The temperature dependence of the crystal thickness of LD80/20 reveals that half-integer-fold crystals can be rather stable, in contrast to the situation in the homopolymers. Relatively low-molecular-weight polymers, such as PEO, polyethylene etc.,[1] form integer-fold crystals and show a stepwise increase of the lamellar crystals with crystallization temperatures. Only at the beginning of the crystallization, noninteger-fold crystals appear due to kinetic reasons, which will subsequently transform into integer-fold ones.[40] In the case of LD80/20, crystals with one and half folds exist for a certain temperature range, stabilized by the D-lactide block. In a diblock copolymer with one crystallizable block, competition between the preferred conformation of each of the blocks, i.e., unfolded chains for the crystallizable component and random-coil chains for the amorphous one, results in an equilibrium degree of chain folding in the crystalline layers.[41,42] As the L-lactide block crystallizes, the D-lactide block becomes highly stretched, which brings the number of possible statistical conformations down. Though a crystal with one and half folds is thermodynamically not stable, compensation by the loss of entropy from the D-lactide block keeps this situation relatively stable within a certain temperature range. As for the LD80/20 sample, the D-lactide block is relatively short (about 6 nm); upon increasing the crystallization temperature further, the frustration of the D-lactide block can be overcome by an increase of the crystal thickness l.

The strong frustration of the amorphous block can stop the increase of the crystal thickness with crystallization temperature as demonstrated by the behavior of LD66/33. Because LD66/33 crystallizes at high temperatures only in the stereocomplex form, at least half of the L-lactide block has to remain amorphous. An increase of the crystal thickness with temperature would result in a crowding effect of cilia or brushes on the top and bottom surface.[43] If the gain in free energy by increasing the crystal thickness is comparable with or less than the loss of entropy from the amorphous part, it is impossible to form a thicker crystal. This indeed is the general trend in short-chain block copolymers with one crystallizable block,[44−46] which deviate from the theoretical predictions for folded-chain crystals in thermodynamic equilibrium.[41,42]

Conclusions

On the basis of small- and wide-angle X-ray scattering measurements, a schematic phase diagram of poly(L-lactide-*b*-D-lactide) diblock copolymers has been established. In the symmetric situation, only the stereocomplex form is obtained over the whole range of crystallization temperatures, while the strongly asymmetric form LD80/20 grows only into homocrystallites. For an intermediate block ratio (66/33), a coexistence region of stereocomplex and homocrystalline phases exists at low crystallization temperatures. The appearance of stereocomplex and/or homocrystalline modifications is determined not only by the thermodynamic driving force but also by the kinetic route. A linear relation with crystallization temperature is observed for the symmetric diblock copolymer (50/50), following the general rule for homopolymers. The lamellar spacing of the asymmetric diblock copolymers shows stepwise increases with temperature, corresponding to integer and half-integer folds. For the intermediate block ratio, the surface crowding effect slows down a further increase of lamellar spacing at high temperatures.

Acknowledgment. The authors thank M. Al-Hussein, W. Hu, D. Lambreva, and I. Sikharulidze (Amsterdam) for valuable discussions. This work is part of the Softlink research program of the "Stichting voor Fundamenteel Onderzoek der Materie" (FOM), which is financially supported by the "Nederlandse Organisatie voor Wetenschappelijk Onderzoek" (NWO).

References and Notes

(1) Ungar, G.; Zeng, X. B. *Chem. Rev.* **2001**, *101*, 4157.
(2) Ungar, G.; Stejny, J.; Keller, A.; Bidd, I.; Whiting, M. C. *Science* **1985**, *229*, 386.
(3) Cheng, S. Z. D.; Chen, J. H.; Zhang, A. Q.; Heberer, D. P. *J. Polym. Sci., Part B: Polym. Phys.* **1991**, *29*, 299.
(4) Jones, N. A.; Sikorski, P.; Atkins, E. D. T.; Hill, M. J. *Macromolecules* **2000**, *3*, 4146.
(5) Ungar, G.; Mandal, P.; Higgs, P. G.; de Silva, D. S. M.; Boda, E.; Chen, C. M. *Phys. Rev. Lett.* **2000**, *85*, 4397.
(6) Zhu, L.; et al. *Phys. Rev. Lett.* **2001**, *86*, 6030.
(7) Loo, Y. L.; Register, R. A.; Ryan, A. J. *Phys. Rev. Lett.* **2000**, *84*, 4120.
(8) de Jeu, W. H. In *Polymer Crystallization: Observations, Concepts and Interpretations*; Reiter, G., Sommer, J. U., Eds.; Springer: Berlin, 2004; Chapter 11, p 196.
(9) Hamley, I. W. *The Physics of Block Copolymers*; Oxford University Press: Oxford, 1998.
(10) Lee, S.-W.; Chen, E.-Q.; Zhang, A.; Yoon, Y.; Moon, B.-S.; Lee, S.; Harris, F. W.; Cheng, S. Z. D.; von Meerwall, E. D.; Hsiao, B. S.; Verma, R.; Lando, J. B. *Macromolecules* **1996**, *29*, 8816.
(11) Hosier, I. L.; Bassett, D. C. *Polymer* **2002**, *43*, 5959.
(12) Cooke, J.; Viras, K.; Yu, G. E.; Sun, T.; Yonemitsu, T.; Ryan, A. J.; Price, C.; Booth, C. *Macromolecules* **1998**, *31*, 3030.
(13) Trzebiatowski, T.; Drager, M.; Strobl, G. R. *Makromol. Chem.* **1982**, *183*, 731.
(14) Lotz, B. *Eur. Phys. J.* **2000**, *E3*, 185.
(15) Slager, J.; Domb, A. J. *Adv. Drug Deli. Rev.* **2003**, *55*, 549.
(16) Ikada, Y.; Jamshidi, K.; Tsuji, H.; Hyon, S. H. *Macromolecules* **1987**, *20*, 904.
(17) Tsuji, H.; Ikada, Y. *Macromolecules* **1992**, *25*, 5719.
(18) Tsuji, H.; Ikada, Y. *Macromolecules* **1993**, *26*, 6918.
(19) Brizzolara, D.; Cantow, H. J.; Diederichs, K.; Keller, E.; Domb, A. J. *Macromolecules* **1996**, *29*, 191.
(20) Cartier, L.; Okihara, T.; Lotz, B. *Macromolecules* **1997**, *30*, 6313.
(21) Sarasua, J. R.; Prud'homme, R. E.; Wisniewski, M.; Borgne, A. L.; Spassky, N. *Macromolecules* **1998**, *31*, 3895.
(22) Baratian, S.; Hall, E. S.; Lin, J. S.; Xu, R.; Runt, J. *Macromolecules* **2001**, *34*, 4857.
(23) Uhrich, K. E.; Cannizzaro, S. M.; Langer, R. S.; Shakesheff, K. M. *Chem. Rev.* **1999**, *99*, 3181.
(24) Drumright, R. E.; Gruber, P. R.; Henton, D. E. *Adv. Mater.* **2000**, *12*, 1841.

(25) Fisher, E. W.; Stersel,; Wegner, H. J. *Kolloid Z. Z. Polym.* **1973**, *251*, 980.
(26) Yui, N.; Dijkstra, P. J.; Feijen, J. *Makromol. Chem.* **1990**, *191*, 481.
(27) Tsuji, H.; Ikada, Y. *Macromol. Chem. Phys.* **1996**, *197*, 3483.
(28) Spinu, M.; Jackson, C.; Keating, M. Y.; Gardner, K. H. *J. Macromol. Sci., Pure Appl. Chem.* **1996**, *A33*, 1497.
(29) Spassky, N.; Pluta, C.; Simic, V.; Thiam, M.; Wisniewski, M. *Macromol. Symp.* **1998**, *128*, 39.
(30) Zhong, Z. Y.; Dijkstra, P. J.; Feijen, J. *Angew. Chem., Int. Ed.* **2002**, *41*, 4510.
(31) Zhong, Z. Y.; Dijkstra, P. J.; Birg, C.; Westerhausen, M.; Feijen, J. *Macromolecules* **2001**, *34*, 3863.
(32) Zhong, Z. Y.; Schneiderbauer, S.; Dijkstra, P. J.; Westerhausen, M.; Feijen, J. *J. Polym. Environ.* **2001**, *9*, 31.
(33) Vonk, C.; Kortleve, G. *Kolloid Z. Z. Polym.* **1967**, *220*, 19.
(34) Strobl, G. R.; Schneider, M. *J. Polym. Sci., Polym. Phys. Ed.* **1980**, *18*, 1343.
(35) Goderis, B.; Reynaers, H.; Koch, M. H. J.; Mathot, V. B. F. *J. Polym. Sci., Part B: Polym. Phys.* **1999**, *37*, 1715.
(36) Sawai, D.; Takahashi, K.; Sasashige, A.; Kanamoto, T.; Hyon, S. H. *Macromolecules* **2003**, *36*, 3601.
(37) Wunderlich, B. *Macromolecular Physics*; Academic Press: New York, 1973; Vol. 2.
(38) Cheng, S. Z. D.; Zhu, L.; Li. C. Y.; Honigfort, P. S.; Keller, A. *Therm. Acta* **1999**, *332*, 105.
(39) Hoffman, J. D.; Weeks, J. J. *J. Res. Natl. Bur. Stand.* **1962**, *A66*, 13.
(40) Cheng, S. Z. D.; Zhang, A.; Barley, J. S.; Chen, J.; Habenschuss, A.; Zschack, P. R. *Macromolecules* **1991**, *24*, 3937.
(41) DiMarzio, E. A.; Guttman, C. M.; Hoffmann, J. D. *Macromolecules* **1980**, *13*, 1194.
(42) Whitmore, M. D.; Noolandi, J. *Macromolecules* **1988**, *21*, 1482.
(43) Halperin, A.; Tirrell, M.; Lodge, T. P. *Adv. Polym. Sci.* **1992**, *100*, 31.
(44) Li L. B.; Lambreva, D.; de Jeu, W. H. *J. Macromol. Sci., Phys.* **2004**, *B43*, 59.
(45) Hong, S.; MacKnight, W. J.; Russell, T. P.; Gido, S. P. *Macromolecules* **2001**, *34*, 2876.
(46) Hong, S.; Yang, L. Z.; MacKnight, W. J.; Gido, S. P. *Macromolecules* **2001**, *34*, 7009.

MA049077O